

Determination of photo conversion efficiency of nanotubular titanium oxide photo-electrochemical cell for solar hydrogen generation

K.S. Raja, V.K. Mahajan, M. Misra *

Metallurgical Engineering, Mail stop 388, University of Nevada, Reno, NV 89557, USA

Received 24 October 2005; received in revised form 7 December 2005; accepted 8 December 2005

Available online 20 January 2006

Abstract

Anodized and annealed titanium oxide nanotubes show enhanced photo activity and can be used as photo anodes for water electrolysis in hydrogen generation. Application of an external potential to the photo anode is required for enhancement of the photocurrent. This additional electrical energy input complicates the photo conversion efficiency calculation. In this investigation, the photo-electrochemical behavior of anodized titanium oxide nanotubular arrays have been characterized in various electrolytes. Increase in the applied potential increased the photocurrent under illumination with visible light. A simple experimental method for calculating the photo conversion efficiency has been proposed. According to this method, the potential difference between the photo anode and cathode is measured with and without light illumination. The product of the photocurrent and the increase in potential due to light irradiation is considered as the net power output. The photocurrent and the conversion efficiency increased with increase in the pH of the electrolyte. TiO₂ nanotubular arrays annealed at 350 °C for 6 h in nitrogen atmosphere showed a maximum photo conversion efficiency of ~4% in 1 M KOH electrolyte and ~3% in 3.5 wt.% sodium chloride solution. The results indicate that nanotubular TiO₂ can be potentially used for the photo electrolysis of seawater to generate hydrogen.

© 2006 Elsevier B.V. All rights reserved.

Keywords: Solar hydrogen generation; Titanium oxide nanotubes; Photo conversion efficiency; Photo anode

1. Introduction

Fujishima and Honda [1] first demonstrated in 1972 that water could be electrolyzed by irradiating an n-type rutile photo anode with solar energy and hydrogen could be produced at the photo cathode in an electrochemical cell. This fascinating discovery initiated a number of investigations in search of more suitable semiconductor materials for the photo splitting of water [2]. For efficient electrolysis of water the photosensitive material should satisfy three basic requirements [3,4]: (1) the electronic band gap should be low so that most of the solar light spectra can be used for photo excitation; (2) band edges of the semiconductor should be conveniently located for easy electron and hole transfers with respect to the H₂/H₂O and H₂O/O₂ energy levels; and (3) the semiconductor should be stable against photo-corrosion in the electrolyte. Among the available photosensitive semiconductor materials, TiO₂ is considered more stable against

photocorrosion even though the band gap is about 3–3.2 eV [2,3]. This larger band gap requires a higher energy of light, predominantly in the UV part of the solar spectrum, for photoexcitation of electron–hole pairs. Therefore, only 3–5% of the solar energy can be used for conversion into photocurrent. In order to increase the photocurrent output, an external potential is generally applied [5]. The supply of external electrical energy reduces the photo conversion efficiency.

Use of nano-structured semiconductor materials has been considered to enhance the photogeneration of hydrogen owing to high surface area and improved charge separation kinetics [6]. Higher photoconversion efficiency has been reported for dye sensitized nanocrystalline TiO₂ solar cells [7,8]. Quantum confinement was considered to occur in the nano-size materials, which could alter the band gap leading to enhanced light absorption [9]. It was suggested that instead of the 3D configuration of nano particles, fabrication of vertical standing nano-wires of TiO₂ could improve the photo conversion efficiency [5]. Anodization of titanium metal substrate in acidified fluoride solution results in formation of ordered vertical standing arrays of TiO₂ nanotubes [10–12]. As the semiconductor nanotubes

* Corresponding author. Tel.: +1 775 784 1603; fax: +1 775 327 5059.
E-mail address: misra@unr.edu (M. Misra).

grow on the Ti metal substrate, a well-defined Schottky type contact is naturally obtained. The vertically-oriented nanotubes can give an easy path for electron transport to the metal substrate. The nanotubes are configured such a way that both inner and outer surface areas of the nanotubes are exposed to the electrolyte, which could facilitate faster hole transport for oxygen evolution during water electrolysis by minimizing the diffusion length by half of the wall thickness of the nanotubes. Further it is envisaged that internal reflections within the TiO₂ nanotubes could enhance the light absorption [13].

The photo conversion efficiency of water electrolysis is calculated based on the following relation [14]:

$$\eta = \frac{J_{\text{ph}} \times E_{\text{rev}}}{I_0} \times 100 \quad (1)$$

where J_{ph} is the photocurrent density; E_{rev} the reversible potential for water electrolysis which is 1.23 V versus standard hydrogen electrode and I_0 the intensity of incident light. If external potential is used the efficiency has been calculated as [3,5]:

$$\eta = \frac{J_{\text{ph}} \times (E_{\text{rev}} - E_{\text{app}})}{I_0} \times 100 \quad (2)$$

where $E_{\text{app}} = E_{\text{meas}} - E_{\text{oc}}$; E_{meas} the potential applied to photo anode versus a reference electrode; E_{oc} the open circuit potential of photo anode under illumination.

When the E_{rev} is considered only as 1.23 V, the theoretical value based on the thermodynamic data, a negative efficiency could be calculated even though a photocurrent is measured at some applied potentials. As the value of the photocurrent is generally orders of magnitude higher than the dark current observed at the corresponding applied potentials, calculation of the negative efficiency of the photo conversion is considered unrealistic. Therefore, a different approach for calculation of the photoconversion efficiency is required under external electrical energy input conditions.

Khan and Akikusha [15] considered an overpotential of 0.5 V for water electrolysis and took $E_{\text{rev}} = 1.73$ in their calculation. However, their calculations involved conversion of the potentials to values corresponding to pH 0. This conversion step may not be necessary, as the theoretical potential difference for water electrolysis at 25 °C remains a constant at 1.23 V irrespective of the pH or reference electrode used. This is not the individual potential of either anode or cathode versus a reference electrode but potential difference between the anode and cathode.

In most of the reports [3,5,13,16] on solar water electrolysis, a parabolic relation between the applied potential and the photo conversion efficiency was observed with almost zero efficiency both at the open circuit potential and the applied potential of 1.23 V. Even though the photocurrent increases with increase in applied potentials, efficiency calculations based on Eq. (2) would still yield negative efficiencies. Therefore, the literature reported efficiency calculations do not represent the actual solar water electrolysis using semiconductors under external potential conditions. In fact, to the best of our knowledge, no investigation has explicitly reported the potential difference between the photo anode and cathode using a three-electrode cell configuration. Only the potential of either the photo anode or cathode has

been measured with respect to a reference electrode [3,5,16,17]. Nozik [18] individually reported the potential of the anode and the cathode with reference to a saturated calomel electrode. As indicated earlier, a theoretical minimum potential difference of 1.23 V (without considering overpotential) should be maintained between anode and cathode for water splitting. Illumination of a photo anode or cathode aids development of the potential difference and decreases the external electrical energy needed to develop the required potential for water electrolysis. It should be noted that when the potential difference between the anode and cathode exceeds the required value, the excess energy could be dissipated as heat energy and would increase the temperature of the electrolyte. Increased temperature decreases the energy required for water electrolysis. Therefore, the increase in applied potential may not result in a negative efficiency as depicted by other reports. The foregoing discussions indicate that the potential difference between the photo anode and cathode should be known for efficiency calculations. In this investigation, the photo-electrochemical behavior of nanotubular TiO₂ photo anodes has been characterized based on the potential between the photo anode and cathode.

2. Experimental

sixteen millimetre discs were punched out from a stock of Ti foil (0.2 mm thick, 99.9% purity, ESPI-metals, Ashland, OR, USA) and secured in a PTFE holder exposing only 0.7 cm² area to the electrolyte. Nanotubular TiO₂ arrays were formed by anodization of the Ti foils in electrolyte solution of 0.5 M H₃PO₄ + 0.14 NaF + 0.1 M NaNO₃.

A two-electrode configuration was used for anodization. A flag shaped Pt electrode served as the cathode. The anodization was carried out at 20 V. Initially the potential was ramped at a rate of 0.1 V s⁻¹ from the open circuit potential to the final anodization potential of 20 V. The anodization current was monitored continuously. During anodization, a magnetic stirrer continuously stirred the solution. After an initial increase–decrease transient, the current reached a steady state value. The anodization was stopped after 20 min of reaching a steady state current value in lower pH electrolytes. The total anodization time was typically about 45 min.

The anodized specimens were annealed in nitrogen atmosphere at 350–500 °C for 1–6 h. Electronic band gap values of the TiO₂ samples were measured from the optical absorption spectra using a UV–vis spectrometer (Model: UV-2401 PC, Shimadzu Corporation, Kyoto, Japan). The morphology of the nanotubes were observed using a field-effect scanning electron microscope (Hitachi, Model:S-4700).

Experiments on hydrogen generation by photo-electrolysis of water were carried out in a glass cell with photo-anode (nanotubular TiO₂ specimen) and cathode (platinum foil) compartments. The compartments were connected by a fine porous glass frit. The reference electrode (Ag/AgCl) was placed closer to the anode using a salt bridge (saturated KCl)-Luggin probe capillary. The cell was provided with a 60 mm diameter quartz window for light incidence. Electrolytes used were: 1 M NaOH, 1 M KOH (pH ~ 14), 0.5 M H₂SO₄ (pH ~ 0.3) and 3.5 wt.%

NaCl (pH \sim 7.2) aqueous solutions. Electrolytes were prepared using reagent grade chemicals and doubly distilled water. No aeration or de-aeration was carried out to purge out dissolved gases in the electrolyte. A computer-controlled potentiostat (Model: SI 1286, Schlumberger, Farnborough, England) was employed to control the potential and record the photocurrent generated. A 300 W solar simulator (Model: 69911, Newport-Oriel Instruments, Stratford, CT, USA) was used as a light source. The light at the 160 W power level was passed through an AM1.5 filter which allowed wavelengths only between 400 and 700 nm to be incident upon the photo-anode. The intensity of the light was measured by a radiant power and energy meter (Model 70260, Newport Corporation, Stratford, CT, USA). Taking into account the losses due to reflection and absorption at various media such as the glass window and the immersion distance (>100 mm) of sample in the electrolyte, etc., the incidence light intensity on the sample is considered as 87 mW cm^{-2} . The samples were anodically polarized at a scan rate of 5 mV s^{-1} under illumination and the photocurrent was recorded. While the potential of the photo anode was measured by the saturated Ag/AgCl reference electrode and potentiostat, the potential of the photo-anode and cathode were recorded separately using a 5-digit digital multimeter (Hewlett Packard, Model: 3468A) during polarization under illumination and in the dark.

3. Results and discussion

Anodization in acidified fluoride solution results in formation of a nanotubular structure. In the absence of fluoride ions, only a thin uniform surface oxide film could be observed. Phosphate and nitrate species present in the electrolyte resulted in adsorption of these ions on the walls of the nanotubes. Annealing of the nanotubes in a low oxygen partial pressure resulted in oxygen vacancy states and possible doping of N and P species in TiO_2 lattice. Fig. 1(a) shows the surface morphology of the as-anodized TiO_2 nanotubes. The tubes are of 70–100 nm in diameter and 400–500 nm in length as observed in Fig. 1(b), which is the side view of the nanotubular array. In the as-anodized condition the nanotubes have an amorphous structure as observed from the X-ray diffraction results (figure not shown). Annealing of the nanotubular arrays at 350°C for 6 h in a nitrogen atmosphere resulted in the transformation of the amorphous phase into anatase, but did not alter the morphology of the nanostructure. Other researchers also reported similar results [16,19].

Fig. 2 shows the optical absorbance spectra of as anodized and annealed TiO_2 nanotubes. In the as-anodized condition, the major absorbance occurred at less than 400 nm and an absorbance tail could be observed at longer wavelengths. Annealing of the nanotubes at 350°C for 6 h was found to increase the absorbance of lower energy light as minor absorbance peaks could be observed at about 390, 430, and 500 nm wavelengths. By extending the tangent line of the major absorbance curve to intercept the wavelength axis at zero absorbance, one can get an idea about the band gap of the material as illustrated in Fig. 2. The band gap of the as-anodized TiO_2 can be considered to be 3.17 eV and annealed TiO_2 nanotubes showed a lower band gap of 2.9 eV. The band gap value and

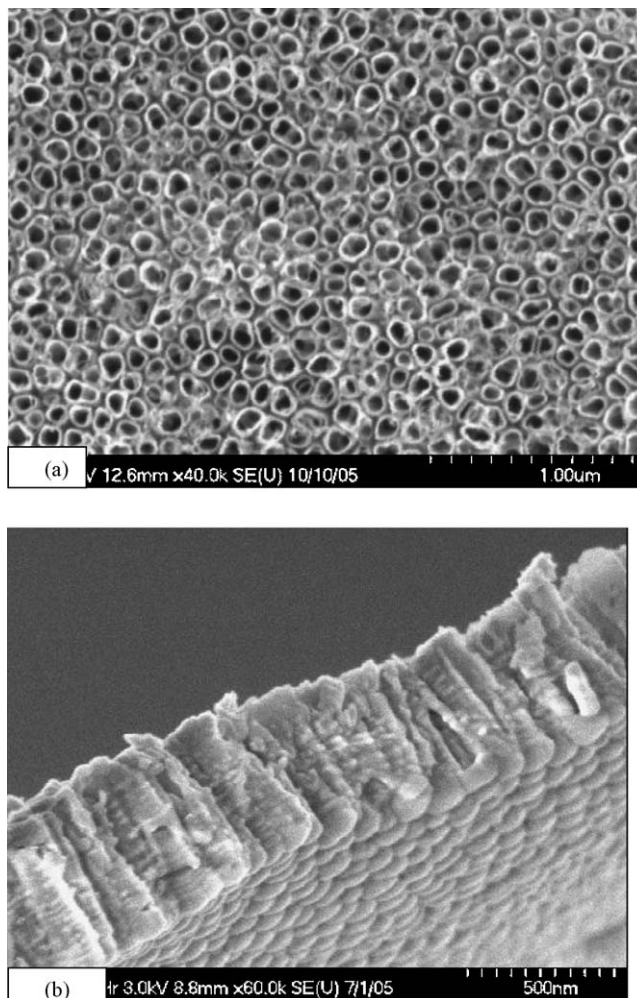


Fig. 1. Morphology of vertically oriented arrays of anodized titanium oxide nanotubes: (a) top view of the surface and (b) side view showing the cross section of the tubes. The tubes were mechanically removed from the Ti substrate. The scalloped barrier film at the bottom surface is also seen.

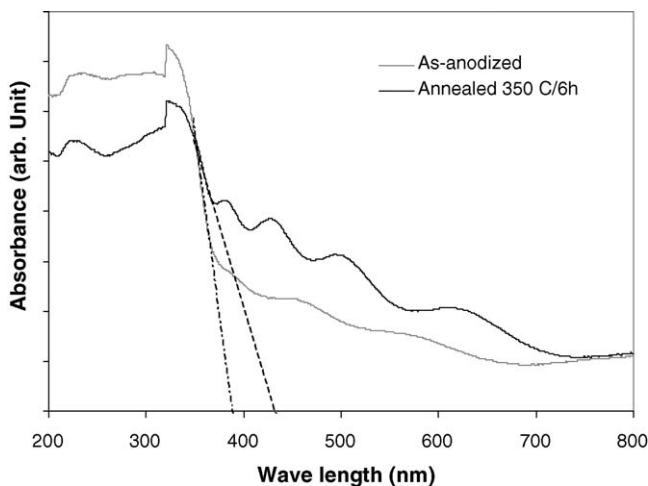


Fig. 2. Optical absorbance spectra of TiO_2 ordered nanotubular anodized in $0.5 \text{ M H}_3\text{PO}_4 + 0.14 \text{ M NaF} + 0.1 \text{ M NaNO}_3$ solution at 20 V for 45 min. Annealing was carried out at 350°C in nitrogen atmosphere for 6 h.

the absorbance characteristics of the annealed nanotubes suggest a better photo activity than that of as-anodized nanotubes and conventional bulk-TiO₂ as well. The increased absorbance of the annealed TiO₂ nanotubes could be attributed to the possible oxygen vacancies generated during annealing at low oxygen partial pressure. In addition to the oxygen vacancy states creating donor levels in the band gap as reported by Cronemeyer [20], band gap states due to the lattice diffusion of P and N species, were introduced during the anodization step and also could be attributed to the absorption tails at higher wavelengths. Minor absorbance peaks observed in the annealed samples could be associated with different levels of band gap states introduced by these species. Based on XPS measurements, Ghicov et al. [21] reported a significant amount of phosphorous species in the TiO₂ nanotubes formed by a similar anodization procedure. Asahi et al. [22] calculated the density of states (DOS) for the doping of carbon, nitrogen and phosphorous in the anatase TiO₂ crystal and considered that the states introduced by carbon and phosphorous substitutions were too deep for overlapping with TiO₂ band gaps. However, increased photo activity of the carbon-doped TiO₂ nanotubes has been well documented [23,24]. Li et al. [23] argued that the observed increase in photo activity of carbon doped TiO₂ did not contradict the theoretical prediction of Asahi et al. [22], as the carbon was present as carbonate, not as a substituted oxygen sub-lattice. Similarly, incorporation of phosphorous species also can be considered to increase the photo activity of TiO₂.

Fig. 3(a) shows the photocurrent and dark current plots of as anodized TiO₂ nanotubes in 1 M KOH solution as a function of potential applied to the photo anode with reference to a Ag/AgCl reference electrode. The photocurrent increased with increase in applied potential to the anode. The potential developed between the photo anode (nanotubular TiO₂) and the cathode (Pt electrode) is also included in Fig. 3(a). The increase in photo current was associated with the increase in the potential between the anode and cathode. Fig. 3(b) compares the potential (between anode and cathode) developed under illumination with that in the dark as a function of the potential applied to the anode. Using a three-electrode configuration and a potentiostat, the potential of the anode was varied with reference to a standard reference electrode (in this investigation it was Ag/AgCl in saturated KCl). However, the photo current due to light excitation (electrons generated by photo excitation) flows from the photo anode to the cathode. There is no current flow in the reference electrode. Therefore, comparison of the potentials between the photo-anode and cathode with and without light illumination would give a better picture of the photo conversion efficiency of the semiconductor material. In the as-anodized condition, the difference in potential, ΔE (defined as the potential increase due to light illumination) was almost a constant at lower applied potentials and increased at higher applied potentials (>1 V versus Ag/AgCl) and the maximum value was about 0.5 V.

Fig. 4 shows the photocurrent behavior of TiO₂ nanotubes annealed at two different conditions, 350 °C for 6 h and 500 °C for 6 h in nitrogen atmosphere. The electrolyte was 1 M NaOH solution. Both the samples showed almost the same behavior. The photo current increased steeply at lower applied poten-

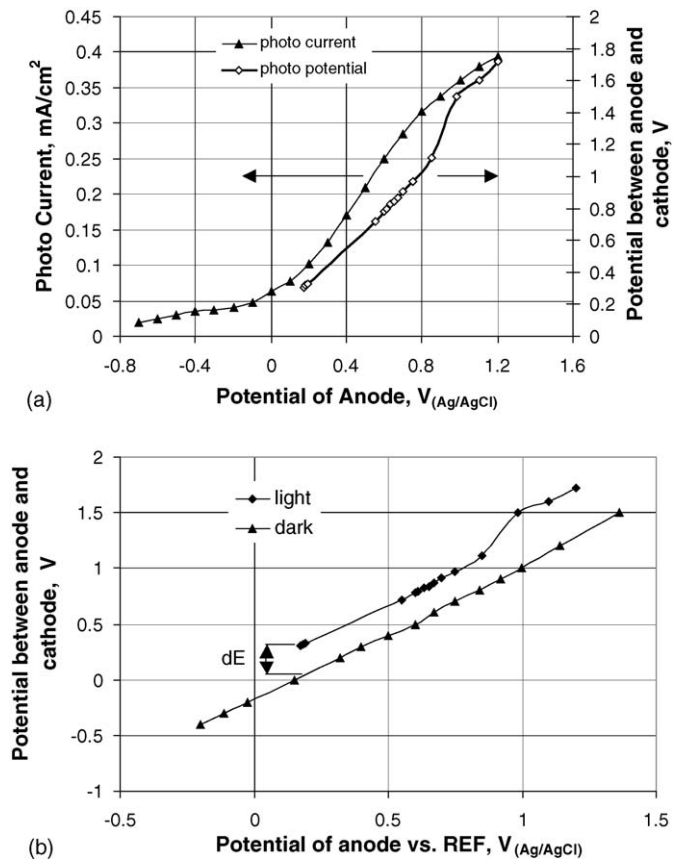


Fig. 3. (a) Photo current density of TiO₂ nanotubes in as-anodized condition as a function of potential applied to the anode. Photo-potential (secondary Y-axis) is the measure potential between the anode and cathode. The electrolyte was 1 M KOH; (b) potential between anode (as-anodized TiO₂ nanotubes) and cathode (Pt) developed with and without light illumination as a function of potential applied to the anode. The electrolyte was 1 M KOH. ΔE (dE) is the increase in potential due to light excitation.

tials and after reaching about -0.2 V versus Ag/AgCl, the current showed almost a saturation behavior. Samples annealed at 350 °C showed better photo activity than those annealed at 500 °C. The optical absorbance spectra also supported the photo current results (not shown in the figure). The reason for

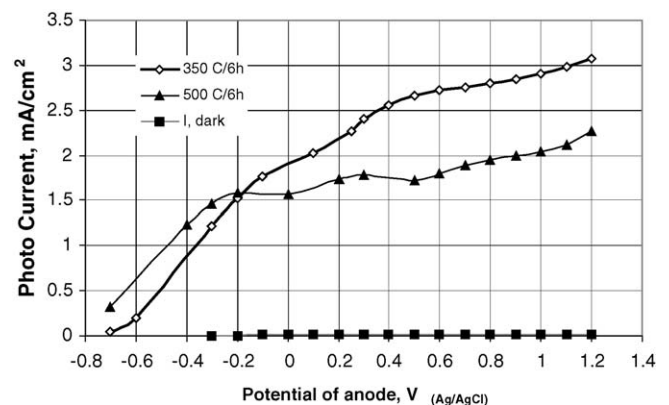


Fig. 4. Photocurrent generated by annealed nanotubular TiO₂ at 350 and 500 °C for 6 h. The electrolyte was 1 M NaOH. Samples were illuminated simulating AM 1.5 condition.

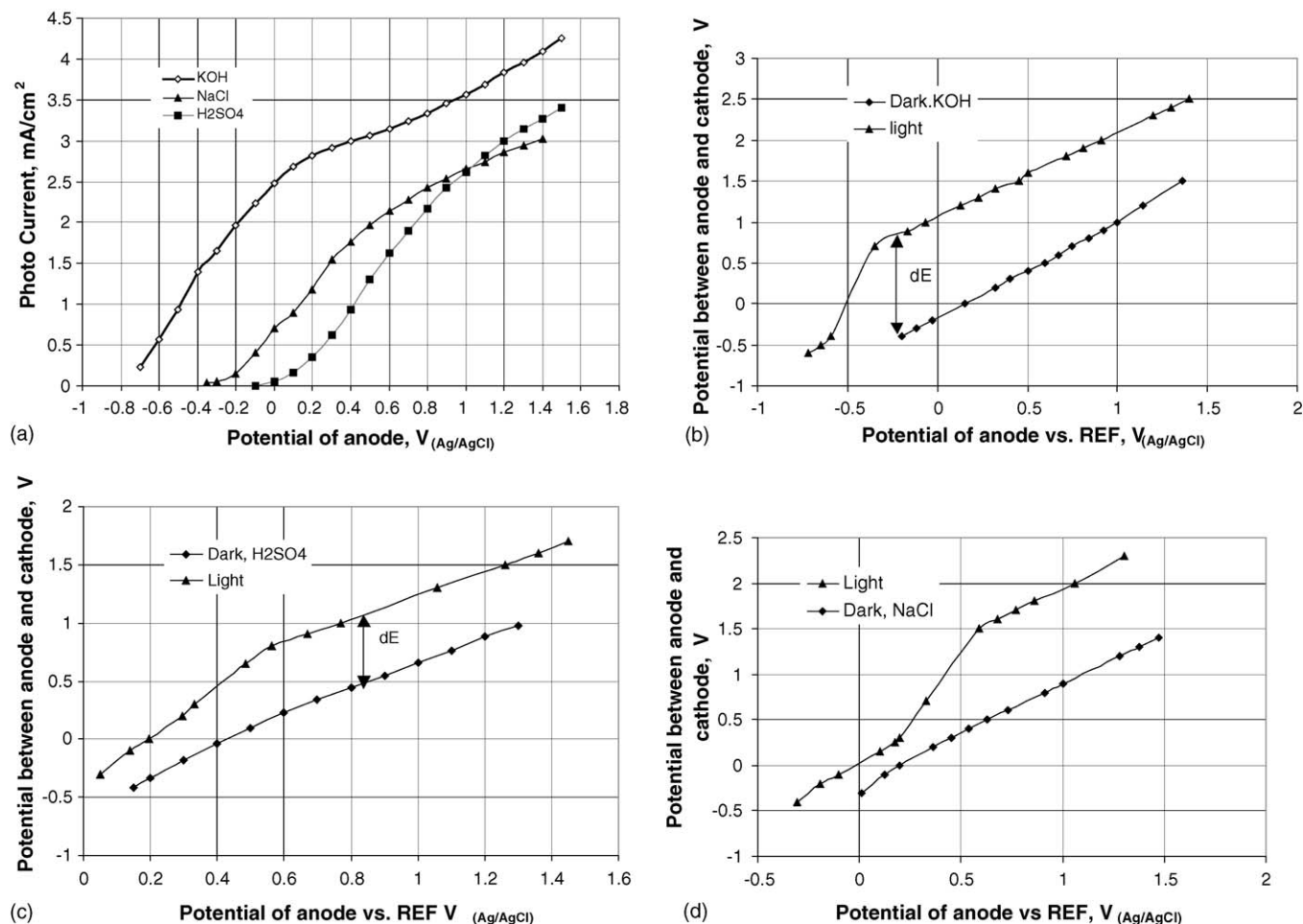


Fig. 5. (a) Photocurrent density of annealed (350 °C for 6 h in N₂) TiO₂ nanotubular arrays in different electrolytes as a function of potential applied to the photoanode; (b) potential between anode (annealed TiO₂ nanotubes) and cathode (Pt) developed with and without light illumination as a function of potential applied to the anode. The electrolyte was 1 M KOH. ΔE (dE) is the increase in potential due to light excitation; (c) potential between anode (annealed TiO₂ nanotubes) and cathode (Pt) developed with and without light illumination as a function of potential applied to the anode. The electrolyte was 0.5 M H₂SO₄. ΔE (dE) is the increase in potential due to light excitation; (d) potential between anode (annealed TiO₂ nanotubes) and cathode (Pt) developed with and without light illumination as a function of potential applied to the anode. The electrolyte was 3.5 wt.% NaCl.

marginally inferior photo activity of the samples annealed at 500 °C is not understood at this time. As the samples annealed at 350 °C showed a better photo activity, only these samples were investigated further in different electrolytes to determine the hydrogen generation behavior.

Fig. 5(a) illustrates the photo-electrochemical behavior of annealed TiO₂ nanotubular arrays (annealed at 350 °C for 6 h in N₂) in different electrolytes. The photocurrent was higher in 1 M KOH as compared to that in 1 M NaOH electrolyte (Fig. 4). The reason for the decreased photo current in the NaOH solution could be attributed to formation of sodium titanate nano-rings on the surface of the photo-anode, which possibly interfered with light absorbance [25]. The current saturation at higher applied potential also could be attributed to the reaction product of NaOH with TiO₂. In other electrolytes, the photocurrent increased with increase in applied potential (Fig. 5(a)) even though the rate of increase varied with potential range. It could be observed that the photocurrent generation decreased with decrease in the pH of the electrolyte at almost all the applied potentials. At higher potentials slightly higher photocurrents

were observed in sulfuric acid solutions than that in NaCl solution. When the photo current was more than 1 mA cm⁻², and the potential difference between the anode and cathode was greater than 1.23 V, hydrogen evolution at the cathode surface could be very clearly observed. Oxygen was evolved at the surface of the photo anode as larger bubbles. Fig. 5(b–d) illustrate the potential of the photo anode and cathode as a function of potential applied to anode in KOH, H₂SO₄ and NaCl solutions, respectively. The potential developed due to illumination was the highest in the KOH solution. The photo potential developed by illumination of the photo anode decreased with decrease in pH of the electrolyte. The maximum value of ΔE in KOH was about 1.26 V, in NaCl solution it was about 1.1 V and in 0.5 M H₂SO₄ it was about 0.6 V. The potential of the anode (nanotubular TiO₂ sample) was measured with reference to an Ag/AgCl reference electrode. When the potential of anode was 0 V versus Ag/AgCl, the measured photocurrent was 2.5 mA cm⁻² as shown in Fig. 5(a). It should be noted that this 0 V versus Ag/AgCl in saturated KCl corresponds to +0.2 V versus standard hydrogen electrode scale and -4.7 eV with reference to vacuum as indicated by solid-state

physics [26]. This 0 V versus Ag/AgCl was not a zero potential between the anode and cathode or between the anode and ground. The potential difference between the anode and cathode was about 1.1 V (Fig. 5(b)) which was sufficient to produce a photo current. Large magnitudes of photo currents were measured at lower potentials as shown in Figs. 4 and 5(a). It should be noted that hydrogen evolution was observed on the cathode surface only when the potential difference between anode and cathode exceeded the theoretical minimum potential of 1.23 V (Fig. 5(b–d)), even though large photo currents were observed at lower potential differences.

Based on the ΔE values, the photo conversion efficiency, η , was calculated using the relation:

$$\eta = \frac{I_{\text{ph}} \times \Delta E}{I_0} \times 100 \quad (3)$$

where I_{ph} is the photo current density in mA cm^{-2} ; ΔE the potential between anode and cathode under illumination—potential between anode and cathode without illumination in V; I_0 the incident light intensity on the photo anode in mW cm^{-2}

Based on the Eq. (3), photo conversion efficiency of annealed nanotubular arrays of TiO_2 in different electrolytes has been plotted as a function of the external potential applied to the photo anode as shown in Fig. 6. It is observed that the efficiency plateaus out after a certain applied potential in all cases. The photo conversion efficiency does not drop to zero or go negative in contrast to the other reports [3,5,16] which is reasonable because when the photo current increases, the efficiency cannot become zero or negative. This is supported by the fact that in the absence of light illumination, application of the same potential to the photo anode resulted in only a microampere range of current. In the efficiency calculations, 100% Faradaic efficiency is assumed for conversion of all photo-current into hydrogen generation. Using this approach, it was observed that the photo conversion efficiency of TiO_2 nanotubular arrays annealed at 350°C for 6 h in nitrogen was about 4% in 1 M KOH and 2.5% in NaCl solution under external applied potentials under visible

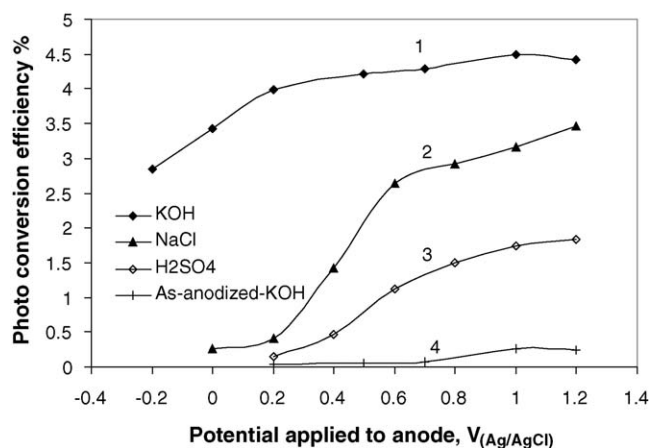


Fig. 6. Photo conversion efficiency of annealed (350°C for 6 h in N_2) TiO_2 nanotubular arrays in different electrolytes as a function of potential applied to the anode. For comparison as-anodized TiO_2 nanotubes in 1 M KOH is included. Legends: (1) annealed TiO_2 in 1 M KOH; (2) annealed TiO_2 in 3.5 wt.% NaCl; (3) annealed TiO_2 in 0.5 M H_2SO_4 and (4) as anodized TiO_2 in 1 M KOH.

light illumination. Nozik [18] observed efficiencies in the range of 3.2–3.4% in 0.1 M KOH with bias potentials of 0.6–1.0 V on single crystal rutile wafers illuminated with 300–400 nm near UV light. In this investigation similar efficiencies were observed with nanotubular TiO_2 irradiated by visible light. Further, Nozik [18] did not describe the method of calculation of efficiency. As-anodized specimens showed conversion efficiencies less than 0.5%.

The difficulty in calculating the photo conversion efficiency using the expression (2) can be further illustrated by considering the energy level interactions of the semiconductor and the electrolyte. Memming [27] analyzed the basic processes involved in the photo electrochemical cells and proposed models to describe the energy levels at the semiconductor–electrolyte interface and to understand the mechanism of photo electrolysis. Based on his model, the differences in photo voltages developed on the n-type nanotubular TiO_2 photo anode in various electrolytes can be explained. When a semiconductor material comes in contact with an electrolyte, the Fermi levels of both phases are equal under equilibrium. In order to achieve the equilibrium, band bending occurs in the semiconductor and there is a potential drop across the space charge layer of the semiconductor in addition to the potential drop across the Helmholtz double layer. The amount of band bending depends on the redox potential of the electrolyte, which determines the Fermi level of the electrolyte. When the electrolyte has a specific redox system such as $\text{Ce}^{4+}/\text{Ce}^{3+}$, $\text{Fe}^{3+}/\text{Fe}^{2+}$, etc., the Fermi level of the electrolyte is fixed at the redox potential of ionic species. In absence of a specific redox system, such as in KOH or NaCl solutions, the Fermi level is not well defined. The Fermi level will be closer to the $\text{O}_2/\text{H}_2\text{O}$ energy level and valence band in case of KOH electrolyte and $\text{H}_2/\text{H}_2\text{O}$ and conduction band in case of 0.5 M H_2SO_4 . Fig. 7(a) and (b) illustrate the TiO_2/KOH system before and after contact in dark conditions. A maximum band bending could be observed if the Fermi level of the electrolyte is closer to the valence band of the material in case of the n-type semiconductor. Accordingly, the band bending will be the maximum with KOH solution as the Fermi level is closer to the $\text{O}_2/\text{H}_2\text{O}$ energy level and the valence band. Following the same principle, the band bending will be a minimum in the sulfuric acid solution and moderate in NaCl solution. The amount of band bending determines the magnitude of the photo potential developed. The condition is similar to that observed on illumination of a solid semiconductor np junction. A maximum photo potential could be observed if the Fermi levels of the semiconductor are closer to the conduction and valence band edges in n-type and p-type semiconductors, respectively [27]. When the semiconductor is illuminated, the energy bands become flat under open circuit condition (because of the electrons reaching the conduction band and the holes reaching the surface/interface) which shifts the energy level corresponding to a photo potential E_{ph} as shown in Fig. 7(c). The shift in photo potential corresponds to a negative shift in open circuit potential in case of n-type semiconductors. Table 1 summarizes typical results for open circuit potentials of nanotubular TiO_2 (annealed at 350°C for 6 h) under dark and illuminated conditions in different electrolytes. As predicted by the analysis of Memming [27], a larger nega-

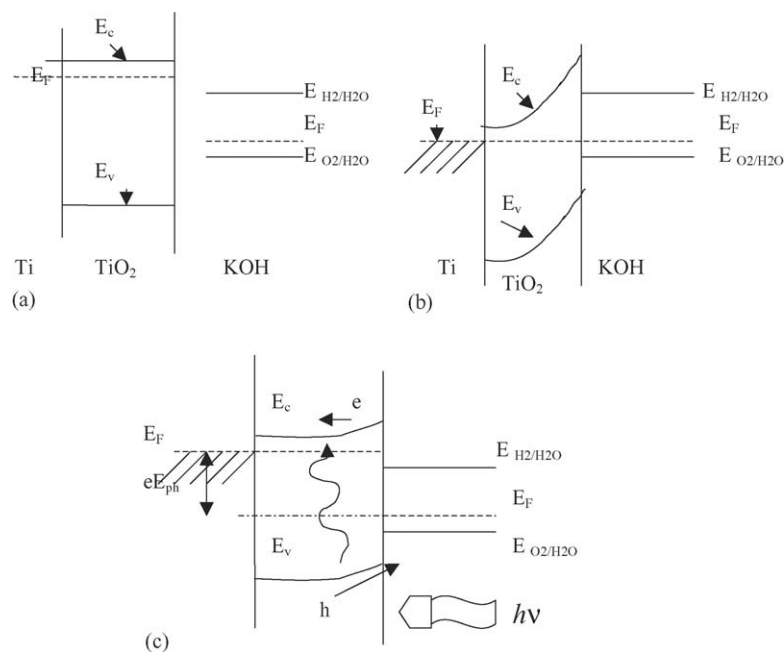


Fig. 7. Schematic illustration of energy levels in the semiconductor and electrolyte interfaces: (a) energy levels of TiO₂ and KOH before contact; (b) after immersion in the electrolyte: Fermi levels are equal; (c) under illumination, a photo potential E_{ph} is developed. E_c is the energy level of conduction band edge, E_v is the energy level of valence band, E_F is the Fermi level, e = electron, h = hole, $h\nu$ is the energy of light.

tive shift in the open circuit potential was observed in the 1 M KOH solution and the photo potential decreased with decrease in pH of the electrolyte. It should be noted that the shift in the potential of the photo anode is opposite to the direction of the bias potential applied. As oxygen evolves on the photo anode, the sample should be anodically polarized. When illuminated, the open circuit potential of the photo anode shifts to a more negative potential. Therefore, when using the expression (2) for efficiency calculation, the term E_{app} becomes extremely large and it appears that the negative-shift in potential due to illumination is disadvantageous. In fact it is not. For n-type materials the photo potential shift will be negative on the standard hydrogen scale and larger the negative shift, more will be the photo activity. It should be noted that these conditions pertain to open circuit conditions. When an external load is connected (such as in the short-circuit condition), the band bending is considered not to change by illumination [27]. Therefore, the term E_{app} in expression (2) need not take the open circuit potential under illumination into account, because the shift in energy level and hence the photo potential will not be effective in unaltered band bending conditions.

Table 1
Open circuit potentials (OCP) of nanotubular TiO₂ (annealed at 350 °C for 6 h) in different electrolytes with and without light illumination

Electrolyte	OCP in dark		OCP in light	
	vs. REF (V _{Ag/AgCl})	vs. Pt cathode (V)	vs. REF (V _{Ag/AgCl})	vs. Pt cathode (V)
1 M KOH	-0.4	-0.38	-0.9	-0.88
0.5 M H ₂ SO ₄	0.11	-0.52	-0.125	-0.76
3.5 wt.% NaCl	-0.19	-0.26	-0.51	-0.54

4. Conclusions

A new and simple method is suggested to determine the photo conversion efficiency of arrays of nanotubular TiO₂ photo anode in a photo electrochemical cell. This method can be extended to other semiconductors also. In this method, the power output by the three-electrode photo-electrochemical cell is calculated by considering the potential increase between the anode and cathode due to light illumination under external applied potential conditions. Using this approach, it was observed that the photo conversion efficiency of TiO₂ nanotubular arrays annealed at 350 °C for 6 h in nitrogen was about 4% in 1 M KOH and 2.5% in NaCl solution under external applied potentials under visible light illumination. The increased photo activity of TiO₂ nanotubular arrays could be attributed to the possible band gap states created by the addition of phosphorous and nitrogen species in the nano-structures during anodization and subsequent nitrogen annealing processes.

Acknowledgements

This work was sponsored by U.S. Department of Energy through DOE Grant no: DE-FC52-98NV13492. The authors gratefully acknowledge the financial support of DOE. The authors thank Mr. Gautam Priyadarshan and Dr. Mo. Ahmedian for their assistance in the experimental work.

References

- [1] A. Fujishima, K. Honda, Nature 238 (1972) 37–38.
- [2] For example J. Nowotny, C.C. Sorrell, T. Bak, L.R. Sheppard, Sol. Energy 78 (2005) 593–602, and references therein.

- [3] S.U.M. Khan, M. Al-Shahry, W.B. Ingel Jr., *Science* 297 (2002) 2243–2245.
- [4] O. Khaselev, J.A. Turner, *Science* 280 (1998) 425–427.
- [5] S.U.M. Khan, T. Sultana, *Sol. Energy Mater. Sol. Cells* 76 (2003) 211–221.
- [6] J. van de Lagemaat, N.-G. Park, A.J. Frank, *J. Phys. Chem., B* 104 (2000) 2044–2052.
- [7] M. Gratzel, *Nature* 414 (2001) 338–344.
- [8] B.A. Gregg, S.-G. Chen, S. Ferrere, *J. Phys. Chem. B* 107 (2003) 3019–3029.
- [9] W.U. Huynh, J.J. Dittmer, A.P. Alvisatos, *Science* 295 (2002) 2425–2427.
- [10] G.K. Mor, O.K. Varghese, M. Paulose, N. Mukherjee, C.A. Grimes, *J. Mater. Res.* 18 (2003) 2588–2591.
- [11] K.S. Raja, M. Misra, K. Paramguru, *Mater. Lett.* 59 (2005) 2137–2141.
- [12] K.S. Raja, M. Misra, K. Paramguru, *Electrochim. Acta* 51 (2005) 154–165.
- [13] G.K. Mor, K. Shankar, M. Paulose, O.K. Varghese, C.A. Grimes, *Nanotechnology* 5 (2005) 191–195.
- [14] S. Licht, *Electrochem. Commun.* 4 (2002) 790–795.
- [15] S.U.M. Khan, J. Akikusha, *J. Phys. Chem. B* 103 (1999) 7184–7189.
- [16] G.K. Mor, K. Shankar, O.K. Varghese, C.A. Grimes, *J. Mater. Res.* 19 (2004) 2989–2996.
- [17] C. Santato, M. Ulmann, J. Augustynski, *J. Phys. Chem. B* 105 (2001) 936–940.
- [18] A.J. Nozik, *Nature* 257 (1975) 383–385.
- [19] O.K. Varghese, D. Gong, M. Paulose, C.A. Grimes, E.C. Dickey, *J. Mater. Res.* 18 (2003) 156–165.
- [20] D.C. Cronemeyer, *Phys. Rev.* 113 (1959) 1222–1226.
- [21] A. Ghicov, H. Tsuchiya, J. Macak, P. Schmuki, *Electrochem. Commun.* 7 (2005) 505–509.
- [22] R. Asahi, T. Morikawa, T. Ohwaki, K. Aoki, Y. Taga, *Science* 293 (2001) 269–271.
- [23] Y. Li, D.-S. Hwang, N.H. Lee, S.-J. Kim, *Chem. Phys. Lett.* 404 (2005) 25–29.
- [24] S. Sakthivel, H. Kisch, *Angew. Chem. Int. Ed.* 42 (2003) 4908–4911.
- [25] S.-H. Oh, R.R. Finones, C. Daraio, L.-H. Chen, S. Jin, *Biomaterials* 26 (2005) 4938–4943.
- [26] J.O'M. Bockris, K. Uosaki, *J. Electrochem. Soc.* 134 (1977) 1348–1355.
- [27] R. Memming, *Electrochim. Acta* 25 (1980) 77–88.